PROBLEMY MECHATRONIKI
UZBROJENIE, LOTNICTWO, INŻYNIERIA BEZPIECZEŃSTWA

ISSN 2081-5891

8, 1 (27), 2017, 71-88

PROBLEMS OF MECHATRONICS
ARMAMENT, AVIATION, SAFETY ENGINEERING

A Probabilistic Model of Optimising Perforated High-Strength Steel Sheet Assemblies for Impact-Resistant Armour Systems

Wojciech BURIAN[1*], Jarosław MARCISZ[2], Lech STARCZEWSKI[3], Małgorzata WNUK[4]

[1] *Institute of Non-Ferrous Metals, 5 Sowińskiego Street, 44-100 Gliwice, Poland*
[2] *Institute for Ferrous Metallurgy, 12-14 K. Miarki Street, 44-100 Gliwice, Poland*
[3] *Military Institute of Armoured and Motor Vehicle Technologies, 1 Okuniewska Street, 05-070 Sulejówek, Poland*
[4] *MIKANIT, 6 Kalinowej Łąki Street, 01-934 Warsaw, Poland*
[*] *Corresponding author's email address: wojciech.burian@imn.gliwice.pl*

Received by the editorial staff on 26 June 2016.
The reviewed and verified version was received on 30 December 2016.

DOI 10.5604/01.3001.0009.8995

Abstract: This paper presents a concept for optimising an assembly of perforated metal sheets with a probabilistic theory, and the results of testing perforated bainite steel sheets with a nanocrystalline structure. The work presented herein was completed with an assumption of applying the perforated sheets in the design of anti-armour-piercing and anti-HEAT armour systems. The theoretical analysis and experimental research were performed for a 7.62 x 54R B-32 (API) projectile and a PG-7 rocket-propelled grenade.
Keywords: mechanics, impact-resistant shields, nanostructural bainite steel, perforated sheets.

This work has been compiled from the paper presented during the 11th International Armament Conference on Scientific Aspects of Armament and Safety Technology, Ryn, Poland, 19 to 22 September 2016

1. INTRODUCTION

Given the performance requirements applied to armoured vehicles, it is necessary to develop armour systems of shields which are light-weight and have high protective capabilities.

Hence, novel solutions must be continuously developed with the use of advanced materials that provide the required protection level at a low weight, or by means of engineering solutions which employ the interactions between projectiles and armour materials. The current results of the research into the development of three-dimensional or laminated armour designs based on perforated baintite steel sheets with nanocrystalline structures [1] suggest that perforated sheet can significantly reduce the armour weight as compared to impact-resistant protective solutions which are currently in use. An armour system of a suitably arranged perforation pattern, combined with the high strength of the steel, ensures the desired edge effect that contributes to fragmentation of a projectile upon impact. Another advantage of perforation in high-strength protective armour materials is a radical reduction in the propagation of cracks formed by reaction to projectile impact. Perforated high-strength steel sheets have been applied as components (i.e. layers) in armour systems [2-15].

The penetrators of armour-piercing projectiles are usually high-hardness materials rated above 65 HRC. This hardness value is achieved by formation of hard reinforcing particles by heat treatment of the penetrator material. The particles generate high levels of internal stress. The resulting state makes the penetrator material prone to cracking under bending stresses, especially when the latter originate from impact. Numerical simulations [15] and experimental data [1] suggest that the impact of an armour-piercing projectile against a hole edge of a perforated sheet applies a bending moment to the projectile, resulting in a high bending stress of the penetrator and the loss of its integrity, followed by fragmentation. When researching a novel bainite steel grade with a nanocrystalline structure with a strength exceeding 2000 MPa, the projective penetrator striking this material was completely destroyed, even when the penetrating core struck the material at 0° incidence [1]. Nanocrystalline bainite steel features a beneficial combination of strength and plasticity that is uncommon in other steel grades applied in armour systems. The factors critical to the properties of the nanocrystalline bainite steel are its chemical composition and properly adjusted heat treatment, which results in a unique type of nanostructure.

The current research in the field contemplated herein is aimed at developing a manufacturing technology of bainite steel products with properties enabling its application in ballistic armour systems or assemblies with extremely high hardness and abrasion resistance, combined with optimised resistance to cracking under impact loads [16-24].

This paper presents the results of experimental tests and theoretical analyses intended to optimise armour shields made of perforated nanocrystalline bainite steel sheets. The paper also presents the results of firing tests of a 6 mm thick perforated steel sheet with the 7.62 x 54R B-32 (API) projectiles and the PG-7 rocket-propelled grenades.

A theoretical analysis was carried out to ascertain the feasibility of designing a geometric arrangement of the steel sheet perforation pattern that would ensure the maximum attainable level of impact protection at a reduced weight of the armour assembly.

The test object of the research this paper contemplates was a three-dimensional model of a steel composite armour assembly installed on an armoured vehicle steel body plate at a slope of ±17° (see Fig. 1). The armour assembly met the requirements for resistance to impact with 7.62 mm API projectiles and the PG-7 rocket-propelled grenades. The research objective was to reduce the model weight by replacing the inner 6-mm thick solid steel sheets with equally thick perforated steel sheets. The assumption was that the protective performance of the modified three-dimensional armour assembly would retain its protective performance unchanged. The focus of optimisation under the research was the selection of the size and spacing of perforation holes. This optimisation was done for the 7.62 x 54R B-32 (API) projectile. The following function of target was assumed: $^{R}/_{T} = f(m_{min})$, with: R is the perforation hole diameter [mm], T is the perforation hole spacing (i.e. the perforation distance) [mm], m is the surface weight of the perforated steel sheet [kg/m^2]. The optimisation was then based on the results of live-fire ballistic testing of the perforated steel sheets with various R and T values.

2. RESEARCH MATERIAL AND METHODS

The research included perforated steel sheets made of a nanocrystalline bainite steel material developed at the Institute for Ferrous Metallurgy under a proprietary restricted trade mark NANOS-BA®. The 6 mm thick perforated steel sheets were heat treated to provide specific mechanical performance. The tensile strength, ultimate tensile strength, ultimate elongation and Charpy's V impact strength of the tested perforated steel sheets were, respectively, 2020 MPa, 1245 MPa, 13%, and 12 J (as tested at -40°C). Following the final heat treatment cycle, the steel sheets were perforated by boring.

The firing tests were carried out according to the test methodology applied at the PCA-accredited Laboratory of Material Engineering (AB083) at the Military Institute of Armoured and Motor Vehicle Technologies and compliant with the applicable national and international standards and references (i.e. PN-EN 1522 and NATO-STANAG 4569). The ammunition types used in the ballistic tests were the 7.62 x 54R B-32 (API) projectiles and the PG-7 HEAT rocket-propelled grenades. The test ordinance was fired at the test object from a distance of 10 m and 0° incidence. The projectile velocity upon impact was 860 ±10 m/s. The live fire tests with the PG-7 RPG were done with an incidence angle of the projectile to the perforated steel sheet armour panel outer skin at 18.5° incidence. The test methodology followed the technical acceptance procedure for armour panels as applied by armour vehicle manufacturers.

3. RESEARCH RESULTS AND DISCUSSION

The research findings obtained so far [1, 18, 19, 21-24] demonstrated that nanocrystalline bainite steel boasts high protective performance when compared to the widely used martensitic armour steel grades. Perforation of the nanocrystalline bainite steel sheets is intended to improve the resistance to cracking of the latter, especially with a multiple projectile impact and the explosion energy of the PG-7 RPGs, and to reduce the deadweight of the material. The tests were carried out using 6-mm thick perforated nanocrystalline bainite steel sheets. The test objective was to compare the projectile penetrator fragmentation capability of the 6-mm thick perforated nanocrystalline bainite steel sheets to the same performance of the previously tested 8 mm sheets [1].

The same perforated steel sheets were used in an armour panel for protection against PG projectiles. The perforated steel sheets were arranged within the armour panel assembly exactly where the 6 mm solid steel sheet, with the same mechanical strength properties (R_m>2.0 GPa) would crack from the explosion of the PG-7 RPG. Fig. 1 shows examples of photographs of 6 mm perforated steel sheet fragments (with the triangular perforation pattern R5T12, see Fig. 1(A)) made of nanocrystalline bainite steel. The regular triangular perforation pattern (staggered at 60°) is usually identified with R, which denotes the perforation hole diameter in millimetres, and T, which is the centre to centre spacing of any two adjacent perforation holes in millimetres. When the tested steel sheet was fired at with the 7.62 x 54R B-32 (API) projectile aimed at the surface that induced bending stress in the projectile penetrator, the steel sheet was not pierced. The characteristic damage suggests that the projectile penetrator failed upon impact (see Fig. 1(B)). The experimental test results revealed that the 6 mm perforated steel sheet caused fragmentation (critical failure) of the projectile penetrator upon impact at a perforation hole. The tested perforated steel sheet weighed 25% less than the 8 mm perforated steel sheet with an identical perforation pattern.

This reduction value is significant, especially given the overall surface area of a steel armour installed on a vehicle or structure.

(A) (B)

Fig. 1. Example photographs of the tested perforated steel sheet fragments before (A) and after (B) the impact of the 7.62 x 54R B-32 (API) projectile

Figure 2 shows photographs of the solid steel sheet armour panel fragments in the explosion area of a HEAT RPG and the entry point of the superplastic jet. The armour panel version shown in Fig. 2 was built with nanocrystalline bainite steel sheets with a rated mechanical strength of 2.0 GPa.

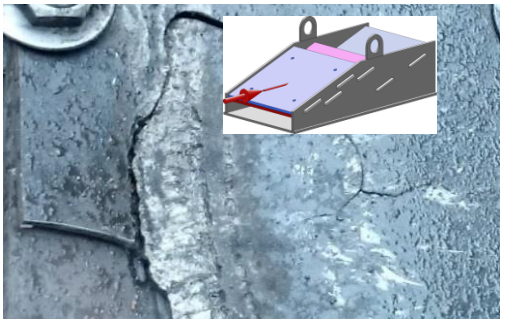

(A)

(B)

Fig. 2. Example photographs of the armoured panel steel sheet fragments at the explosion area of the PG-7 RPG: diagram of (A) the RPG mounting and (B) superplastic jet entry

Both areas revealed cracks in the armour panel sheet. The test results demonstrated that solid bainite steel sheets required resistance to cracking, which would force a reduction of the mechanical strength [23]. To reduce the armour panel deadweight, it was attempted to apply nanocrystalline bainite steel sheets with perforation and a rated mechanical strength exceeding 2.0 GPa. A square perforation pattern R5T12 was used with a hole at each square diagonal intersection. Figure 3 shows the photographs of the armour panel areas similar to those shown in Fig. 2.

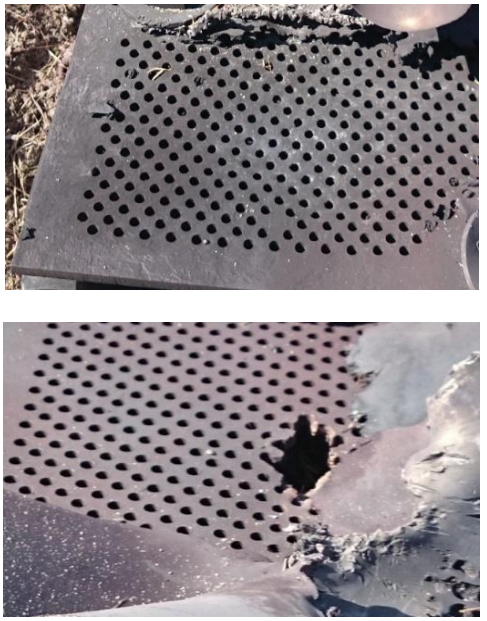

(A)

(B)

Fig. 3. Example photographs of the armoured panel perforated steel sheet fragments at (A) the explosion area of the PG-7 RPG and (B) superplastic jet entry

No cracks were found on the top perforated steel sheet. At the explosion area of the PG-7 RPG, the perforated steel sheet exhibited plastic deformation (comparable to the same damage of the solid sheet), which was partial to a higher resistance to cracking. Both designs of the armour panel (without and with perforation, see Figs. 2 and 3) featured 6-mm thick sheets. The perforation pattern reduced the armour panel layer deadweight by ca. 25%.

The experimental test results demonstrated that armour panel perforated steel sheets made of high-strength steel grades boast a great potential for application in layered or three-dimensional armour shields.

The primary action which prevents penetration of a solid steel sheet with an armour-piercing projectile is to absorb and disperse the projectile energy by plastic deformation (among other factors). In perforated steel sheets, optimum strength also becomes a factor of this action.

Optimum strength induces an asymmetrical force that is applied to the projectile penetrator when it hits near or at a penetration opening.

These impact conditions destabilize the projectile and cause fragmentation of the projectile penetrator, resulting in failure to pierce the armour panel. As for the explosion effects of a PG projectile, the perforation pattern prevents cracking of the steel sheets.

The probability of armour-piercing projectile penetrator failure was calculated for various patterns of regular triangular perforation with circular holes.

This research considered the so-called edge effect Z, a relationship which was the quotient (1) of (i) the diameter difference between the projectile penetrator and the perforation hole, and (ii) the projectile penetrator radius. The edge effect Z value was important due to the level of bending stress applied to the projectile penetrator [9, 25]. It was experimentally determined [13] that the relationship $Z \geq 0{,}35$ must be met to generate a critical bending stress within the projectile penetrator for it to fail and become fragmented.

$$Z = \delta / \frac{D}{2} \geq 0{,}35 \tag{1}$$

$$\delta = D - D_o, \quad r = {}^{D}/_{2} \tag{2}$$

where: D is the projectile penetrator diameter (mm), D_o is the perforation hole diameter (mm), δ is the overlap area width (mm), r is the projectile penetrator radius (mm).

The relationship Z determined the geometry of the projectile penetrator contact with the perforation hole. The geometry imposes conditions that contribute to a change in the projectile penetrator flight trajectory and the generation of significant bending stress. These two factors resulted in the fragmentation or failure of the projectile penetrator. Fig. 4 schematically shows the perforation pattern with the perforation hole diameter R, the perforation pattern T, the surface area with the width δ, which envelopes the area conducive to the fragmentation (failure) of the projectile penetrator, and the surface area S_f an impact at which may pierce the perforated steel sheet. The contemplated calculations considered the 6.0 mm diameter penetrator of the 7.62 x 54R B-32 (API) projectile.

The assumption here was that an impact of the projectile against a penetration hole would cause fragmentation (failure) of the penetrator, since the probability of a penetrator hit coaxial with a perforation hole (without induction of bending stress within the penetrator) is nearly zero.

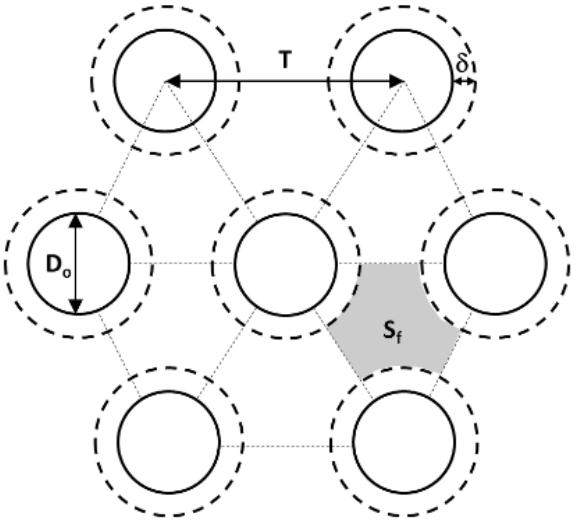

Fig. 4. Diagram of the regular triangular perforation pattern (with a 60° stagger)

With the relationship (1), in first approximation the perforation hole diameter D_o was calculated for a projectile penetrator diameter D, followed by the calculation of the surface area width δ which determines the area conducive to fragmentation (failure) of the projectile penetrator. The related equation (3) was:

$$Z = 2 \cdot \frac{(D - D_o)}{D} \tag{3}$$

This enabled a calculation of the surface area width, which, for a 6.0 mm dia. penetrator (of the 7.62 x 54R B-32 (API) projectile) was 1.05 mm at the perforation hole diameter R of 4.95 mm. Fig. 5 shows the diagram of overlap of the projectile penetrator with a perforation hole. If there was a large difference between the projectile penetrator diameter and the perforation hole diameter (see Fig. 5(A)), the surface area which stabilized the projectile penetrator would prevent induction of bending stress in the penetrator. If the perforation hole diameter was close to the penetrator diameter (see Fig. 5(B)), the surface area which stabilized the projectile penetrator would be largely reduced, while the surface area conducive to penetrator bending stress would remain the same; hence the calculation inputs considered the optimum perforation hole diameter $R_{opt} = D - 0.2$. The optimum perforation hole diameter (R_{opt}) for the 6.0 mm dia. projectile penetrator was 5.8 mm.

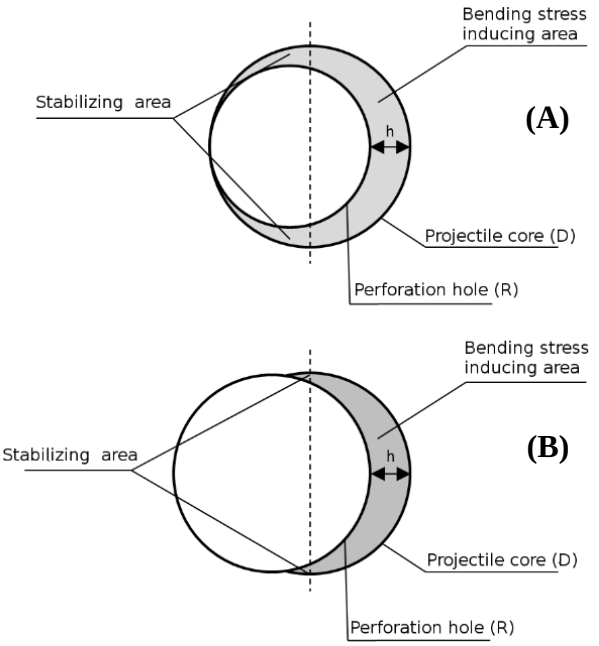

Fig. 5. Diagram of perforated steel sheet hole diameter optimisation

The next step of the calculation was to determine the variance range of the perforation pattern T_{opt}. The T_{opt} minimum and maximum values were determined with the equations (6) and (7), by assuming that the probability of projectile penetration failure in the first shot was 0.99 and 0.50, respectively. The result was the interval of T_{opt} values, which were input to the following calculations:

$$T_{\text{opt}} = \langle 7.57;\ 10.64 \rangle \tag{4}$$

The perforated steel sheet clearance P, which represented the perforated steel sheet weight reduction to the solid steel sheet, was calculated with the relationship:

$$P = \frac{2 \cdot \pi \cdot R_{opt}^2}{T_{opt}^2 \cdot \sqrt{3}} \tag{5}$$

The projectile penetrator fragmentation conducive surface area S_i was calculated with the formula:

$$S_i = \frac{1}{2} \cdot \pi \cdot \left(\frac{R_{opt}}{2} + \delta \right)^2 \tag{6}$$

The projectile penetrator fragmentation (failure) probability *Pn* in the first shot was:

$$\mathrm{Pn}(1) = \frac{\mathrm{N}}{\mathrm{N}} \cdot \left(\frac{\mathrm{S_i}}{\mathrm{S}}\right) \tag{7}$$

with *S* as the surface area between the centres of three adjacent perforation holes and the result $\frac{\mathrm{T}^2\sqrt{3}}{4}$. The projectile penetrator fragmentation (failure) probability in the second shot was:

$$\mathrm{Pn}(2) = \frac{\mathrm{N\text{-}1}}{\mathrm{N}} \cdot \left(\frac{\mathrm{S_i}}{\mathrm{S}}\right)^2 \tag{8}$$

projectile penetrator fragmentation (failure) probability in the *n*th shot was determined with the equation:

$$Pn(n) = \frac{(N-1)(N-2)\cdot\ldots\cdot(N-n+1)}{N^{n-1}} \cdot \left(\frac{S_i}{S}\right)^n = \frac{N!}{N^n \cdot (N-n)!} \cdot \left(\frac{S_i}{S}\right)^n \tag{9}$$

where the factor $\mathrm{Nw} = \frac{\mathrm{N!}}{\mathrm{N^n \cdot (N\text{-}n)!}}$ considered the effect of failure of individual components (i.e. the areas between the centres of three adjacent holes in a triangular configuration) of the perforated steel sheet after the successive shots, and *N* is the number of components (surface areas *S*) on the perforated steel sheet. The calculation was done for 10 shots (*n* = 1..10) and with an assumption that the hit against each perforated steel sheet component has an equal probability for the perforated steel sheets sized 100 x 100 mm and 1000 x 1000 mm. Fig. 6 shows the relationship of the perforated steel sheet clearance *P* and the perforation pattern T_{opt}.

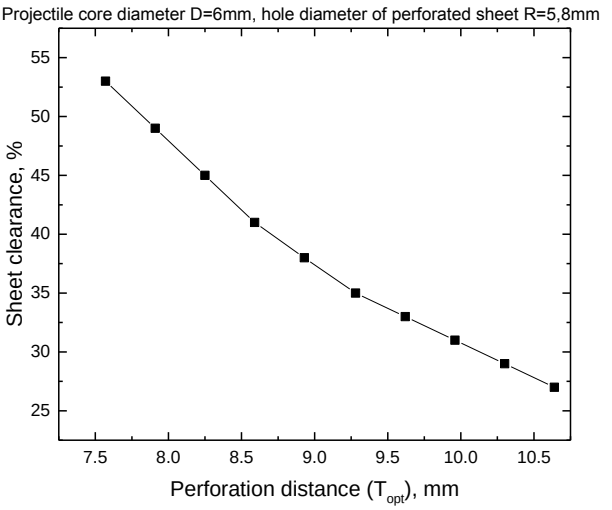

Fig. 6. Calculated relationship of the perforated steel sheet clearance and the perforation distance

The calculation results suggested that the attainable weight reduction of the perforated steel sheet relative to the solid steel sheet of the same material and thickness oscillated between 27 and 53%. Figure 7 presents the results of the projectile penetrator fragmentation probability *Pn* in relation to the perforation pattern T_{opt} and the number of shots for a perforated steel sheet sized 100 x 100 mm. Figure 8 shows the calculation results for the function *Nw* in relation to the perforation pattern T_{opt} and the number of shots *n*. The function described the effect of elimination of the perforated steel sheet components *N* in each successive shot (*N* – is the surface areas *S*). The calculation results suggested that with the minimum perforation pattern T_{opt} the projectile penetrator fragmentation in the 10th shot has a probability of 0.79, provided that there was an equal probability of hit across the entire surface area of the perforated steel sheet.

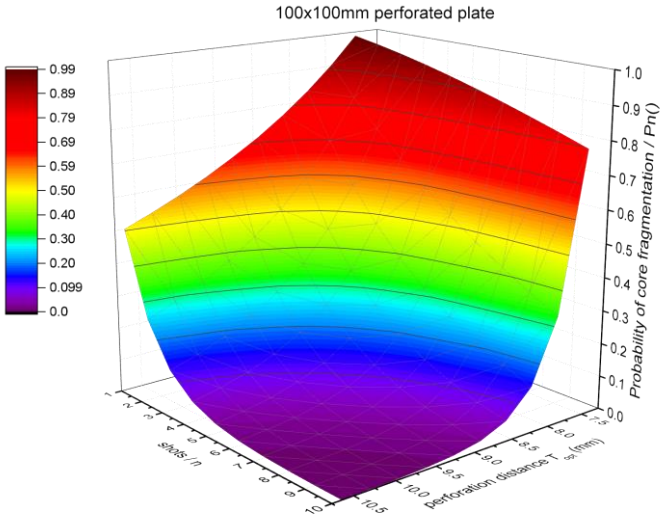

Fig. 7. Calculated probability of projectile penetrator fragmentation (failure) in relation to the perforation distance T_{opt} and the number of shots *n* for the 100 x 100 mm perforated steel sheet

The function *Nw* (see Fig. 8) showed that with the 100 x 100 mm perforated steel sheet with 403 *N* components, the failure of individual components reduces the projectile penetrator fragmentation probability by ca. 0.11 after the 10th shot (at the minimum T_{opt}).

The function of the projectile penetrator fragmentation probability *Pn* was reduced drastically as the perforation pattern T_{opt} was increased. This suggests that the best protective performance was shown by a perforated steel sheet with a low T_{opt}.

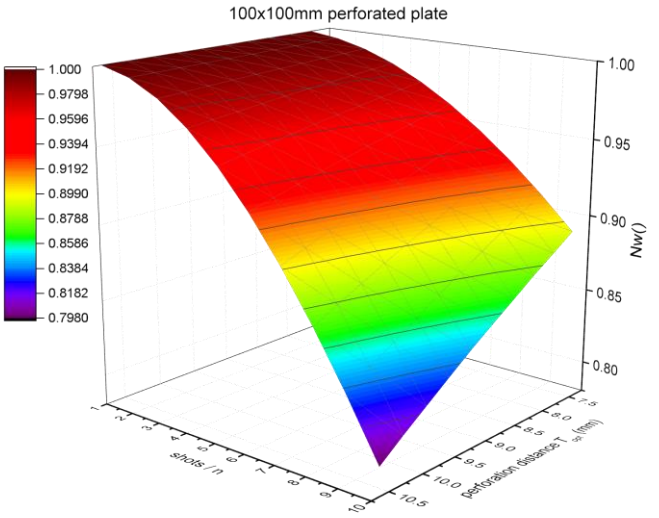

Fig. 8. Calculated *Nw* value of the number of failed perforated steel sheet components in relation to the perforation distance T_{opt} and the number of shots *n* for the 100 x 100 mm perforated steel sheet

Figs. 9 and 10 present the calculation results for the projectile penetrator fragmentation probability *Pn* and the function *Nw* in relation to the perforation pattern T_{opt} and the number of shots *n* for a perforated steel sheet sized 1000 x 1000 mm. There was a distinct difference from the calculation results delivered for the 100 x 100 mm perforated steel sheet.

The 1000 x 1000 mm perforated steel sheet had 40300 *N* components, which increased the projectile penetrator fragmentation probability *Pn* after the 10th shot to 0.88 at the minimum perforation pattern T_{opt}.

The function *Nw* demonstrated that the larger number of components *N* on the perforated steel sheet made the effect of their failure on the protective performance negligible. With the 1000 x 1000 mm perforated steel sheet and the minimum T_{opt}, the *Nw* value after the 10th shot was only 0.001. The results demonstrated that the optimum perforation hole diameter and the perforation raster are critical factors of the protective performance in the design of armour systems based on perforated steel sheets with large numbers of surface area *S* elements.

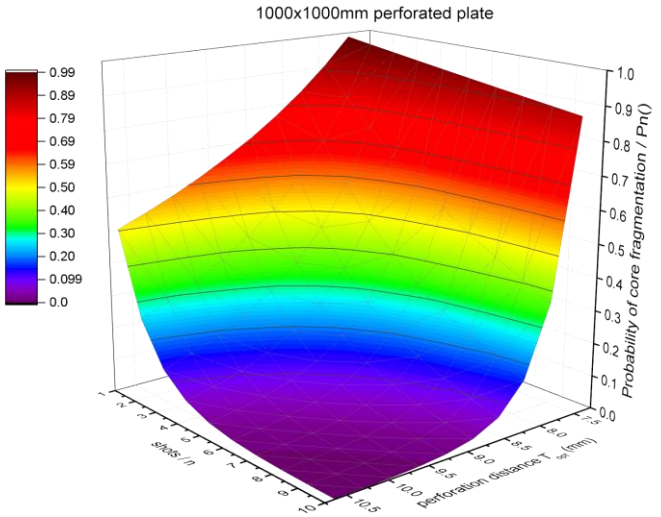

Fig. 9. Calculated probability of projectile penetrator fragmentation (failure) in relation to the perforation distance T_{opt} and the number of shots n for the 1000 x 1000 mm perforated steel sheet

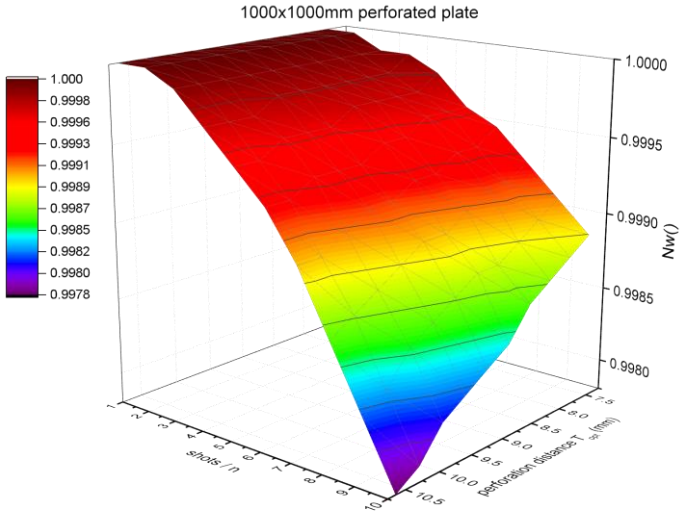

Fig. 10. Calculated *Nw* value of the number of failed perforated steel sheet components in relation to the perforation distance T_{opt} and the number of shots *n* for the 1000 x 1000 mm perforated steel sheet

4. CONCLUSION

The experimental test and theoretical analysis results presented herein demonstrate that the application of perforated sheets made of nanocrystalline high-strength bainite steel in ballistic armour designs will provide high protective capability with a large reduction of armour weight. The probabilistic model proposed herein for optimisation of the perforation pattern geometry can be useful in the design engineering of perforated steel sheet armour systems. The model would require expansion of the thickness range and mechanical properties of the perforated steel sheets.

The live-fire experimental tests done on the 6 mm perforated steel sheets made of nanocrystalline bainite subject to impact of the 7.62 x 54R B-32 (API) projectiles found that an edge effect existed that resulted in failure of penetration. Given the previous live-fire tests of 8 mm thick perforated steel sheets, the armour panel deadweight was reduced by 25%. The application of perforated steel sheets in laminated armour panels demonstrated a high resistance to cracking from exposure to the explosive force of PG rocket-propelled grenades. Research is underway to develop finished systems of perforated steel sheets of high-strength steel grades in order to produce an armour system with a relatively low weight.

The research work has been co-financed by the Polish National Centre for Research and Development under Program INNOTECH, program pathway IN-TECH
(Project no. INNOTECH-K1/IN1/27/150443/NCBR/12, title: „Development of an advanced armour module resistant to the impact effects of HEAT superplastic jets and projectiles"
(Opracowanie nowoczesnej konstrukcji modułu pancerza odpornego na udarowe oddziaływanie strumienia kumulacyjnego i pocisków)

REFERENCES

[1] Burian Wojciech, Jarosław Marcisz, Lech Starczewski. 2015. „Osłony antyudarowe na bazie perforowanych blach ze stali bainitycznej o strukturze nanokrystalicznej". *Problemy techniki uzbrojenia* 136 (4) : 105-123.

[2] Kilic Namik et al. 2014. "Ballistic behavior of high hardness perforated armor plates against 7.62 mm armor piercing projectile". *Materials & Design* 63 : 427-438.

[3] Haque Z. Bazle, Meaghan M. Kearney, John W. Gillespie Jr. 2012. "Advances in protective personnel and vehicle armors" *Recent Pat Mater Sci.* 5 : 103-34.

[4] Ben-Moshe David. 1986. Patent Nr EP 0 209 221 A1. *An armor assembly for armored vehicles*.

[5] Auyer A. Richard, Robert J. Buccellato, Andrew J. Gidynski, Richard M. Ingersol, Needangalam S. Sridharan. 1991. Patent No.: 5,014,593. *Perforatedplatearmor*.

[6] Ravid Moshe, Yoav Hirchberg. 2009. Patent No.: 7,513,186 B2. *Ballisticarmor*.

[7] Norris William J., Craig A. Smith. 2010. Patent No.: WO 2010/036411 A2. *Perforated armor with geometry modified for lighter weight*.

[8] Madhu Vemuri, Balaksrishna T. Bhat. 2011. "Armour protection and affordable protection for futuristic combat vehicles". *Defence Scientific Journal* 61 : 394-402.

[9] Balos Sebastian, Vencislav Grabulov, Leposava Sidjanin, Mladen Pantic, Igor Radisavljevic. 2010. "Geometry mechanical properties and mounting of perforated plates for ballistic application". *Matererials & Design* 31 : 2916-2924.

[10] Radisavljevic Igor, Sebastian Balos, Milutin Nikacevic, Leposava Sidjanin. 2013. "Optimization of geometrical characteristics of perforated plates" *Matererials & Design* 49 : 81-89.

[11] Mishra Bidyapati, Pradipta Kumar Jena, Balaksrishnan Ramankrishna, Vemuri Mahdu, Balaksrishnan T. Bhat, Neha K. Gupta. 2012. "Effect of tempering temperature, plate thickness and presence of holes on ballistic impact behavior and ASB formation of a high strength steel". *Interntional Journal of Impact Engineering* 44 : 17-28.

[12] Mishra Bidyapati, Balaksrishnan Ramankrishna, Jena P.K., Kumar S.V., Vemuri Mahdu, Neha K. Gupta. 2013. "Experimental studies on the effect of size and shape of holes on damage and microstructure of high hardness armour steel plates under ballistic impact". *Matererials & Design* 43 : 17-24.

[13] Howell Ryan, Jonathan S. Montgomery, David C. Van Aken. 2008. Advancements in steel for weight reduction of P900 armor plate. In *Proceedings of 26th army science conference*, Orlando,USA.

[14] Chocron Sidney, Charles E. Anderson, Donald Grosch, Carl H. Popelar. 2001. "Impact of the 7.62 mm APM2 projectile against the edge of a metallic target". *Interntional Journal of Impact Engineering* 25 : 423-437.

[15] Rosenberg Zvi, Yechezkel Ashuach, YehoshuaYeshurun, Erez Dekel. 2009. "On the main mechanism for defeating AP projectiles, long rods and shaped charge jets". *Interntional Journal of Impact Engineering* 36 : 588-596.

[16] Bhadeshia Harry. 2005. *Hard bainite, TMS-The Minerals*, Metals and Materials Society, 1 : 469-484.
[17] Marcisz Jarosław, Bogdan Garbarz, Wojciech Burian, Mariusz Adamczyk, Adam Wiśniewski. 2011. New Generation Maraging Steel and High-Carbon Bainitic Steel for Armours. In *Proceedings of the 26th International Symposium on Ballistics,* Miami, USA, 1595-1606.
[18] Marcisz Jarosław, Bogdan Garbarz, Wojciech Burian, Jerzy Stępień and Lech Starczewski. 2013. Ballistic testing of nano-precipitation hardened and nano-duplex steels. In *Proceedings of the 27th International Symposium on Ballistics,* Freiburg, Germany, 1834-1845.
[19] Patent UP RP No. P394037, 20.05.2014, Patent pending in UP RP No. P396431/2011.
[20] Burian Wojciech, Jarosław Marcisz, Bogdan Garbarz, Lech Starczewski. 2014. "Nanostructured bainite-austenite steel for armours construction". *Archives of Metallurgy and Materials* 59 (3) : 1211-1216.
[21] Marcisz Jarosław, Bogdan Garbarz, Wojciech Burian, Jerzy Stępień, Lech Starczewski, Robert Nyc. 2013. Badania balistyczne blach wykonanych z innowacyjnego gatunku stali bainitycznej NANOS-BA®. W *Materiały XIX Międzynarodowej Konferencji Naukowo-Technicznej: Problemy Rozwoju, Produkcji i Eksploatacji Techniki Uzbrojenia, UZBROJENIE 2013*, Jachranka, Polska, 84.
[22] Garbarz Bogdan, Wojciech Burian. 2014. „Microstructure and Properties of Nanoduplex Bainite-Austenite Steel for Ultra-High-Strength Plates" *Steel Research International* 85 (12) : 1620-1628.
[23] Marcisz Jarosław, Wojciech Burian, Jerzy Stępień, Lech Starczewski, Małgorzata Wnuk. 2014. Stalowo-kompozytowe panele ochronne przeciw pociskom kumulacyjnym (PG) z zastosowaniem blach z nanokrystalicznej stali bainityczno-austenitycznej. W *Materiały X Międzynarodowej Konferencji Uzbrojeniowej*, Ryn, Polska.
[24] Marcisz Jarosław, Wojciech Burian, Jerzy Stępień, Lech Starczewski, Małgorzata Wnuk, Jacek Janiszewski. 2014. Static, dynamic and ballistic properties of bainite-austenite steel for armours. In *Proceedings of the 28th International Symposium on Ballistics,* Atlanta, USA.
[25] Radisavljevic Igor, Sebastian Balos, Milutin Nikacevic, Leposava Sidjanin. 2013. "Optimization of geometrical characteristics of perforated plates". *Materials & Design* 49 : 81-89.

Probabilistyczny model optymalizacji układów perforacji blach z wysokowytrzymałych stali do zastosowań w systemach osłon antyudarowych

Wojciech BURIAN[1, 2], Jarosław MARCISZ[2], Lech STARCZEWSKI[3], Małgorzata WNUK[4]

[1] *Instytut Metali Nieżelaznych, ul. Sowińskiego 5, 44-100 Gliwice, Polska*
[2] *Instytut Metalurgii Żelaza, ul. K. Miarki 12-14, 44-100 Gliwice, Polska*
[3] *Wojskowy Instytut Techniki Pancernej i Samochodowej, ul. Okuniewska 1, 05-070 Sulejówek, Polska*
[4] *MIKANIT, ul. Kalinowej Łąki 6, 01-934 Warszawa, Polska*

Streszczenie. W artykule przedstawiono koncepcję optymalizacji układu perforacji blach na podstawie teorii probabilistycznej oraz wyniki badań blach perforowanych wykonanych ze stali bainitycznej o strukturze nanokrystalicznej. Prace zrealizowano w kierunku zastosowania płyt perforowanych w konstrukcjach osłon przeciwko pociskom przeciwpancernym oraz głowicom kumulacyjnym. Analizy teoretyczne i badania eksperymentalne przeprowadzono dla naboju 7,62 x 54R z pociskiem B-32 oraz granatu PG-7.

Słowa kluczowe: mechanika, osłony antyudarowe, nanostrukturalna stal bainityczna, blachy perforowane